Supporting Information

Aromatic Interaction vs. Hydrogen Bonding in Self-Assembly at the Liquid-Solid Interface

Rico Gutzler*[a], Sophie Lappe[a], Kingsuk Mahata[b], Michael Schmittel[b], Wolfgang M. Heckl[a,c], and Markus Lackinger[a]

Department of Earth and Environmental Sciences and Center for NanoScience (CeNS), Ludwig-Maximilians-University, Theresienstraße 41, 80333 Munich, Germany; Center of Micro and Nanochemistry and Engineering, Organische Chemie I, University Siegen, Adolf-Reichwein-Straße 2, 57068 Siegen, Germany; Deutsches Museum, Museumsinsel 1, 80538 Munich, Germany

Contents

I. Synthesis of Chemical Compound II

4-{2-{3,5-Bis[2-(4-carboxyphenyl)-1-ethynyl]-2,4,6-trimethylphenyl}-1-ethynyl}benzoic acid

Scheme 1

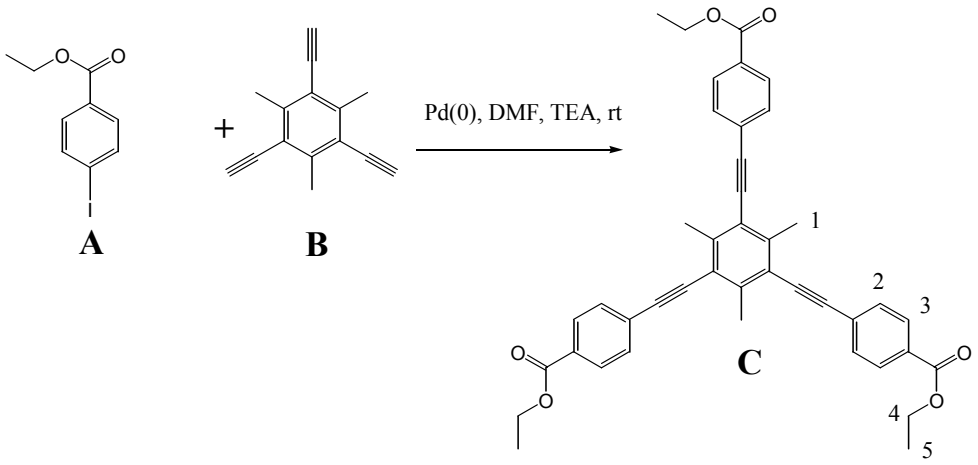

Preparation of C: To a solution of ethyl 4-iodobenzoate (**A**, 1.15 g, 4.16 mmol) in triethylamine (20 mL) and DMF (20 mL), triethynylmesitylene (**B**, 200 mg, 1.04 mmol) and $Pd(PPh_3)_4$ (120 mg, 104 µmol) were added under N_2. The resulting mixture was stirred at room temperature for 20 h. The reaction mixture was dissolved in CH_2Cl_2 (100 mL) and washed with water (2 × 100 mL). The organic phase was dried over $MgSO_4$ and filtered. After removal of the solvents the crude product was purified by column chromatography (silica, ethylacetate:hexane, 1:4) to afford the product as a white solid (490 mg, 77%). MP: 162 °C. IR (KBr): $\tilde{\nu}$ = 3424 (w), 2980 (w), 2203 (w), 17186 (s), 1605 (s), 1506 (w), 1404 (w), 1366 (w), 1271 (s), 1174 (m), 1105 (s), 1019 (m), 854 (m), 767 (s), 694 (w), 526 (w). ^{1}H-NMR (400 MHz, $CDCl_3$): δ = 1.41 (t, *J* = 7.1 Hz, 9H, 5-H), 2.73 (s, 9H, 1-H), 4.40 (q, *J*

= 7.1 Hz, 6H, 4-H), 7.58 (d, *J* = 8.3 Hz, 6H, 2-H), 8.02 (d, *J* = 8.3 Hz, 6H, 3-H). ^{13}C-NMR (100 MHz, $CDCl_3$): δ = 14.4, 20.5, 61.3, 89.6, 97.1, 121.2, 128.0, 129.7, 130.0, 131.4, 143.0, 166.1. Anal calcd for $C_{42}H_{36}O_6$: C, 79.22; H, 5.70; found: C, 79.81; H, 5.69.

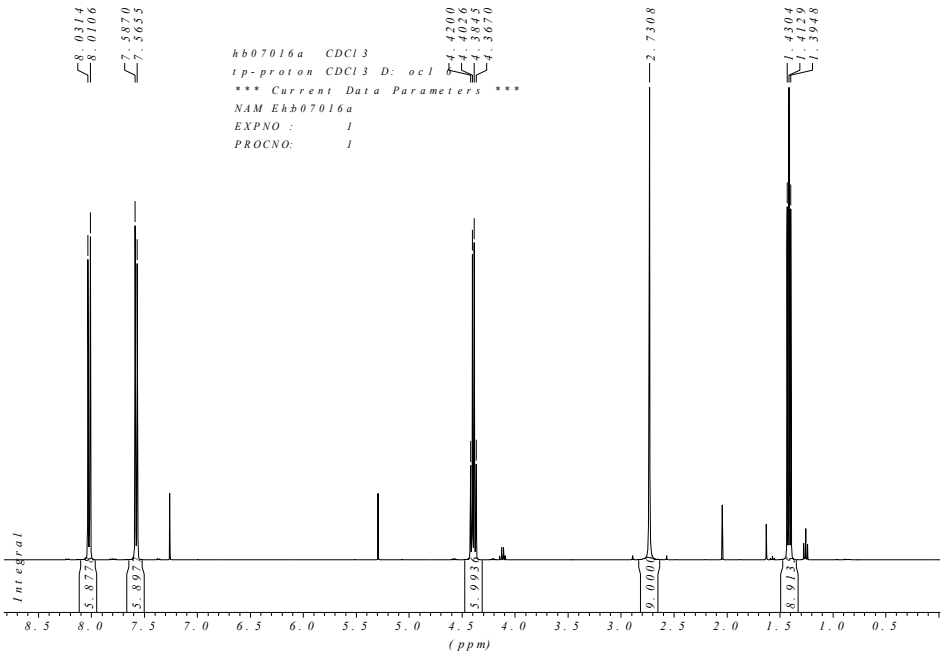

^{1}H-NMR spectrum of compound **C**

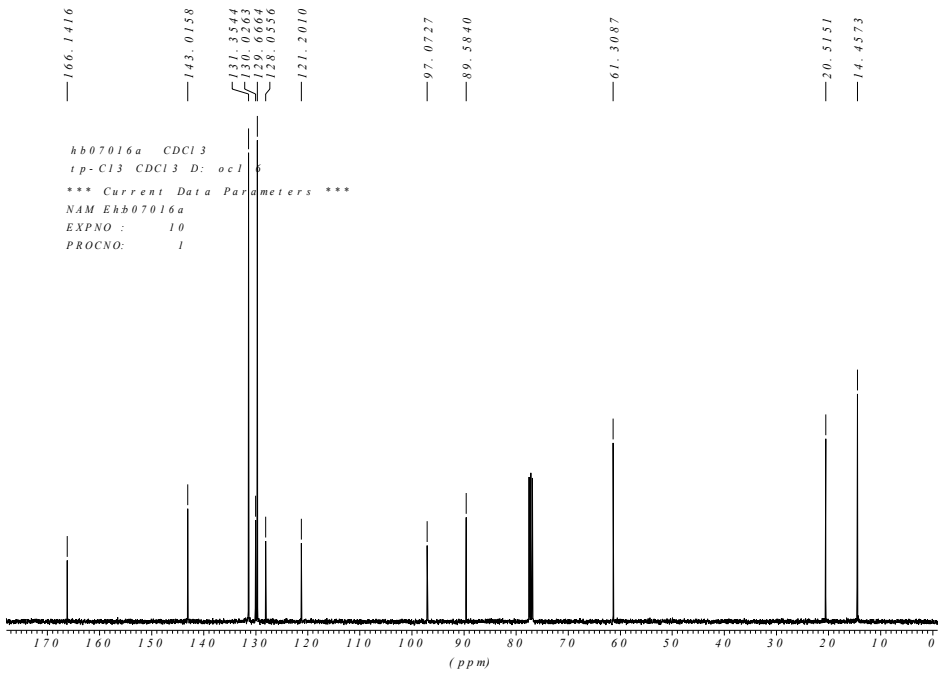

^{13}C-NMR spectrum of compound **C**

Scheme 2

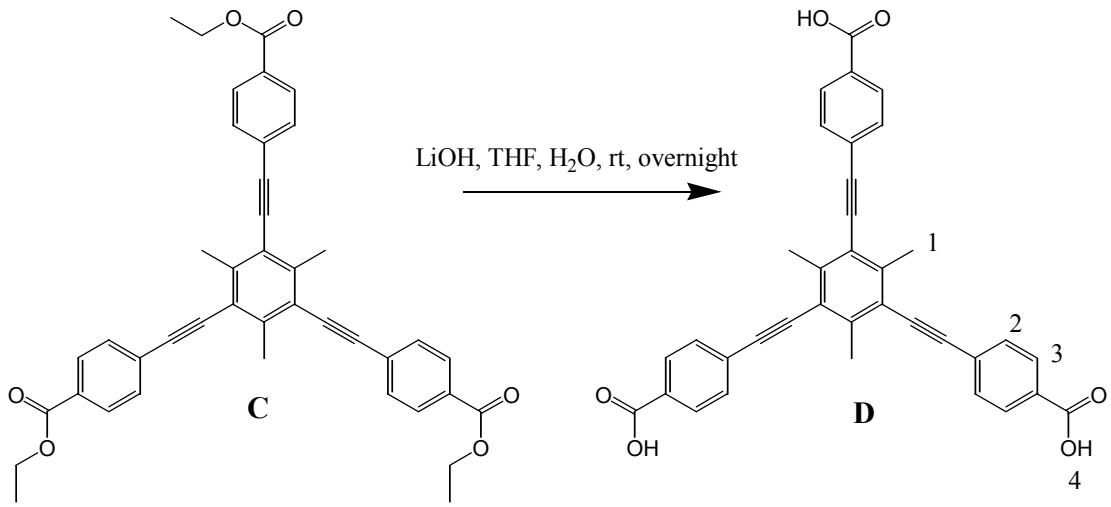

Preparation of D: Ester **C** (430 mg, 675 µmol) was dissolved in a mixture of THF (12 ml) and H_2O (1.8 mL). Then, LiOH monohydrate (568 mg, 13.5 mmol) was added and the mixture was stirred at room temperature while H_2O (6 mL) was added over a period of 1 hour. After the mixture had been stirred at room temperature overnight, 30 mL of THF was added. Then 100 mL of 1 M HCl was added to this solution and the precipitate was filtered by suction. The solid was washed with 100 mL of 1 M HCl and 100mL of acetone to afford product **D** as a white powder (340 mg, 0.615 mmol, 91%). MP: >300 °C. IR (KBr): $\tilde{\nu}$ = 3445 (w), 2850 (w), 2525 (w), 2361 (w), 2200 (w), 1686 (s), 1604 (s), 1558 (m), 1417 (s), 1311 (m), 1275 (s), 1172 (m), 1106 (w), 1015 (w), 854 (m), 768 (s), 690 (w), 551 (w), 510 (w). ^{1}H-NMR (400 MHz, DMSO-d_6): δ = 2.74 (s, 9H, 1-H), 7.72 (d, *J* = 8.3 Hz, 6H, 2-H), 7.99 (d, *J* = 8.3 Hz, 6H, 3-H), 13.22 (br s, 3H, 4-H). ^{13}C-NMR (100 MHz, DMSO-d_6): δ = 20.2, 88.6, 97.1, 120.6, 126.5, 129.6, 130.8, 131.4, 142.6, 166.7. Anal calcd for $C_{36}H_{24}O_6$*1.25H_2O: C, 75.19; H, 4.64; found: C, 75.15; H, 4.40.

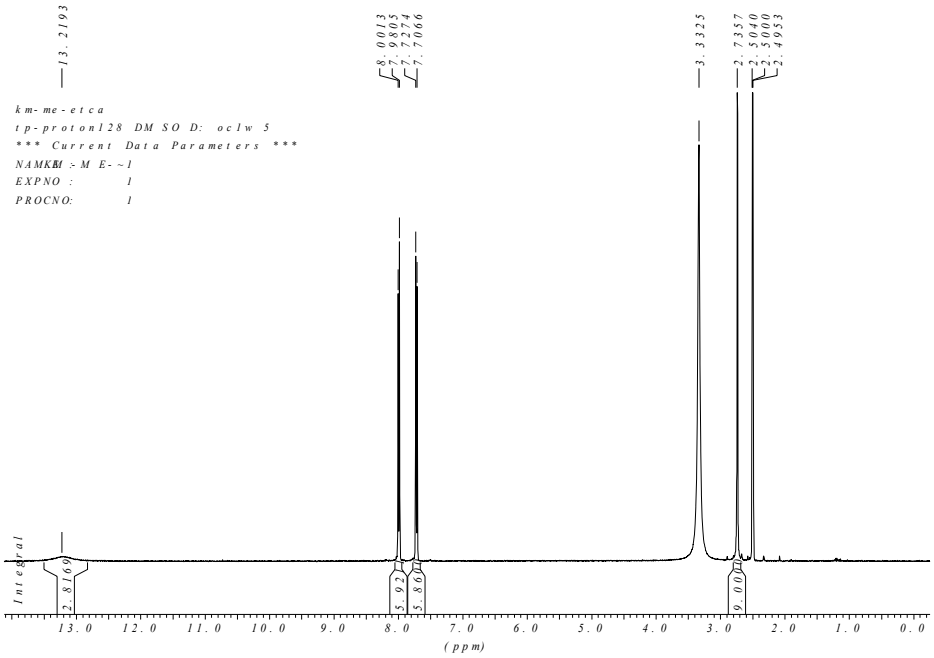

^{1}H-NMR spectrum of compound **D**

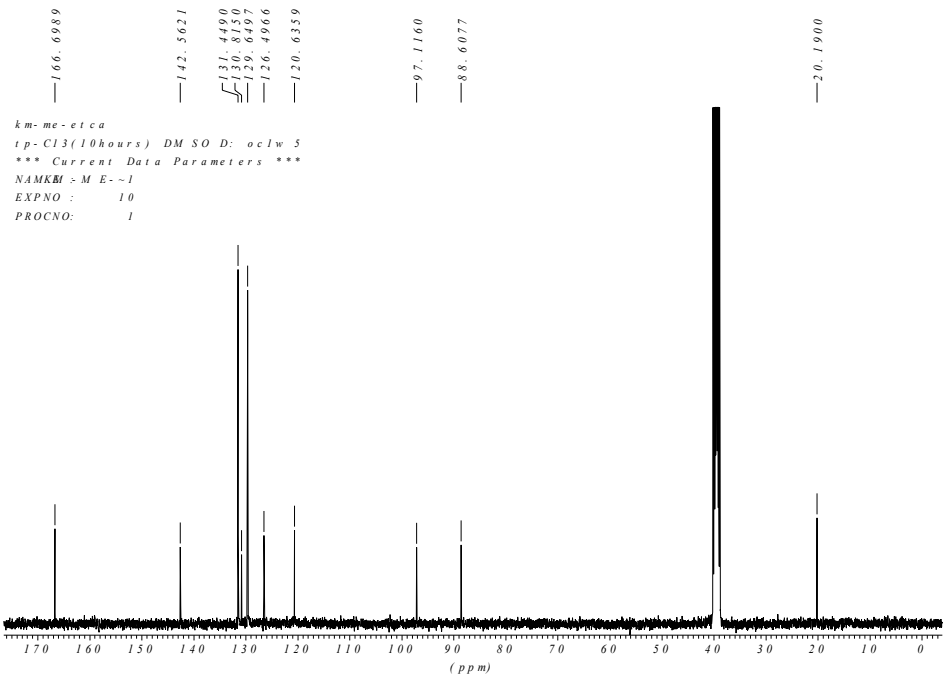

^{13}C-NMR spectrum of compound **D**

II. Experimental details and additional STM topographs

STM experiments were performed with a home-built instrument at ambient temperature (20-25 °C). Solvents were purchased from Aldrich and used as received. STM tips were cut mechanically from platinum/irdium wire (80% Pt / 20% Ir, diameter = 0.25 mm). Molecules **I** and **II** were dissolved in all solvents until saturation. Prior to imaging, a drop (~2.5 μL) of saturated solution was applied to a freshly cleaved (0001) surface of HOPG (Highly Oriented Pyrolytic Graphite). STM experiments were carried out at the liquid-solid interface with the tip immersed into solution in constant-current mode. Atomically resolved graphite images were used for lateral calibration.

UV/vis absorption spectra were recorded with the USB4000 spectrometer from Ocean Optics and a deuterium tungsten lamp as excitation source. Due to high absorbance of the solute molecules a quartz glass cuvette with an optical path length of 1 mm was used. Absorption spectra of pure nonanoic acid were used as a reference.

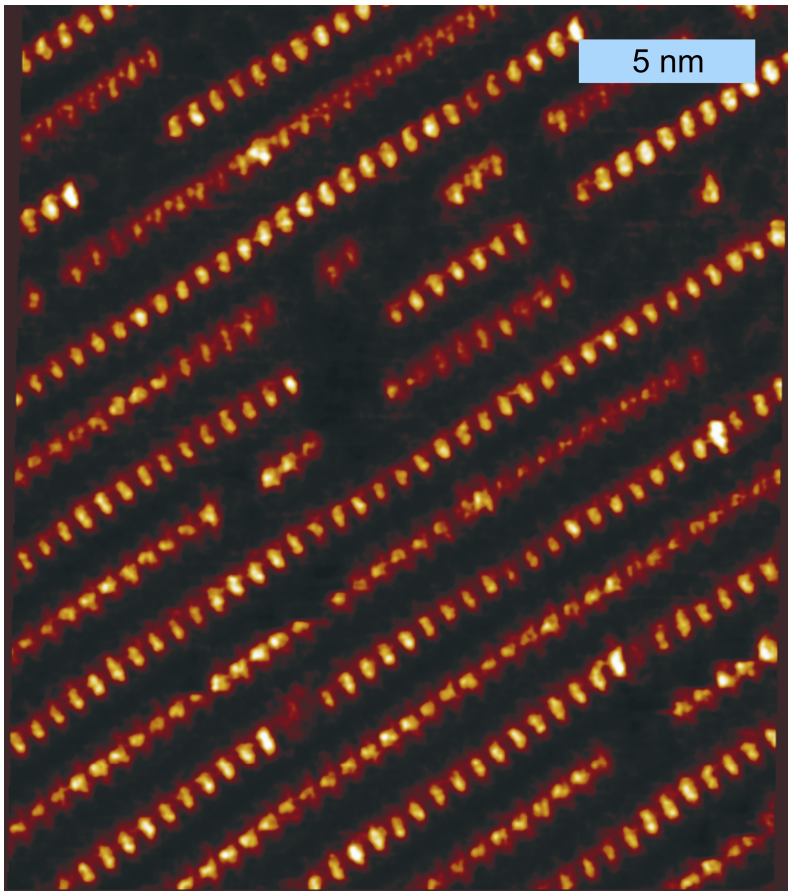

Figure S1. STM topograph of self-assembled monolayers of molecule **I** dissolved in NA (1.2 V; 20 pA). Interrow spacing is 1.9 nm. A high number of defects can be observed and is typical for this self-assembled monolayer.

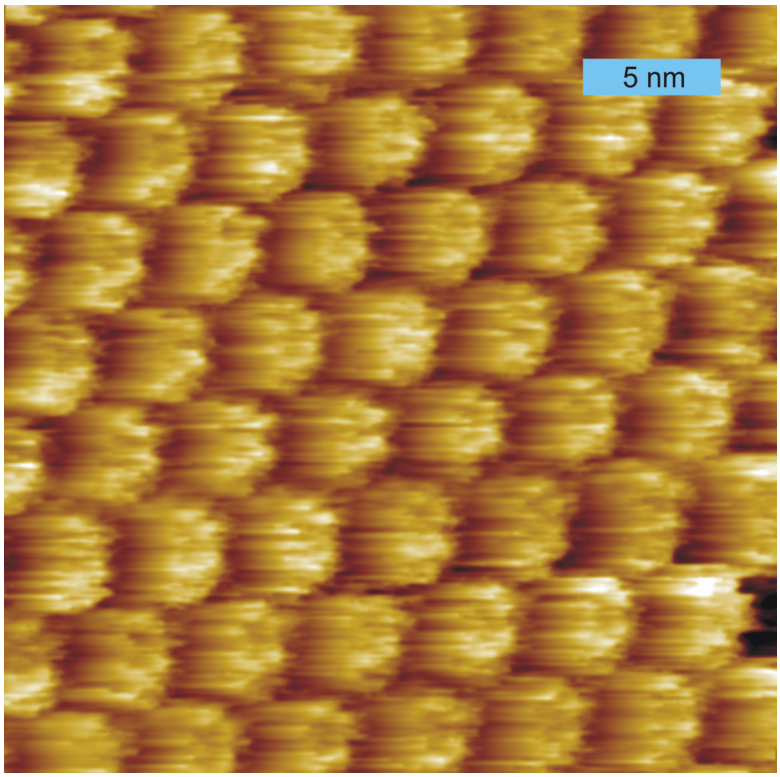

Figure S2. STM topograph of self-assembled monolayers of molecule **I** dissolved in DBB (1.2 V; 100 pA). The lattice parameter of this hexagonal structure accounts to 4.1 nm and is equal to the value of the hexagonal structure of compound **I** in TCB. This class of aromatic nonprotic solvents interacts with the solute through aromatic interactions and is able to break up preformed solute aggregations in solution. Consequently, monomeric adsorption results and the H-bonded chickenwire structure can form.

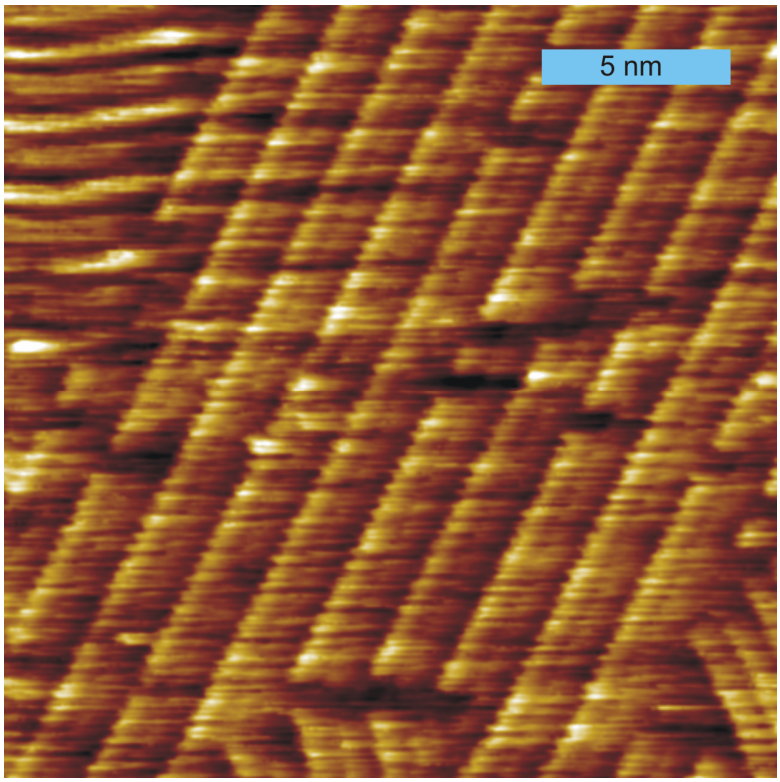

Figure S3. STM topograph of self-assembled monolayers of molecule **I** dissolved in PBA (1.3 V; 23 pA). The same row structure with a row spacing of 1.9 nm is observed in NA. Although the phenyl ring of the solvent might interact with the aromatic system of the solute, the interaction is too weak to cause monomeric dissolution and consequently precipitation of the H-bonded chickenwire structure.

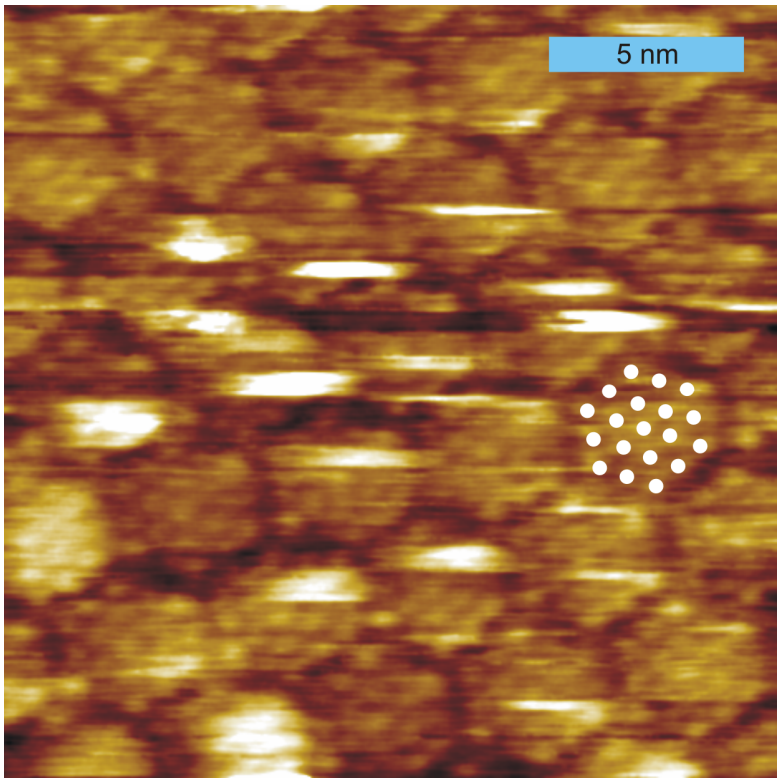

Figure S4. High resolution STM image of self-assembled monolayers of molecule **I** in TCB. Within each cavity 19 bright spots can be identified as indicated by the white dots. The close packed arrangement of the dots exhibits hexagonal symmetry and the size of one dot corresponds to the size of a TCB molecule. This contrast can be explained by planar co-adsorption of 19 solvent molecules within the cavity, thus each bright dot corresponds to one TCB molecule.

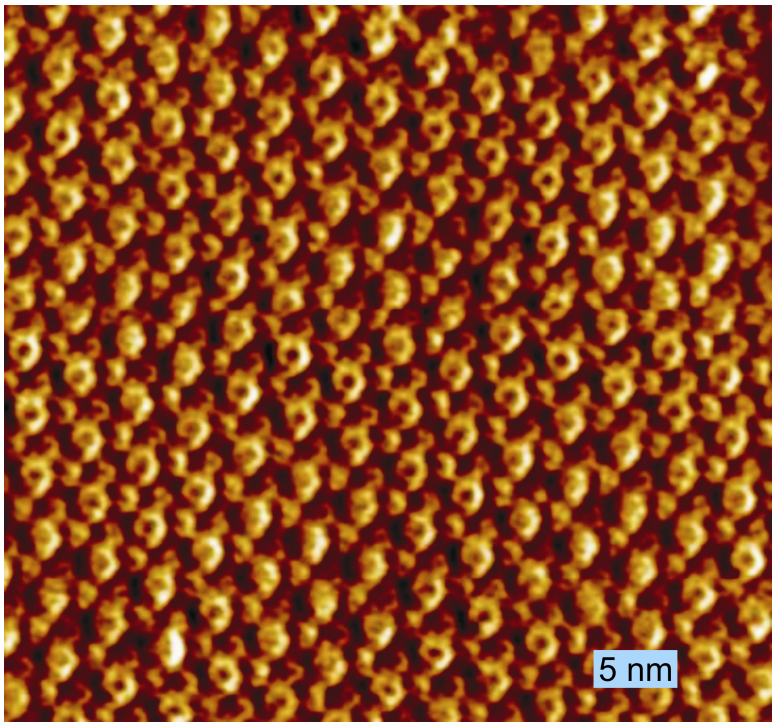

Figure S5. STM topograph of self-assembled monolayer of molecule **II** in TCB (1.1 V; 70 pA). As in Fig. S4, the cavities of the hexagonal arrangement appear brighter than the surrounding molecules **II** themselves. This can be explained by co-adsorption of solvent molecules within the cavities of the open pore network. Molecular resolution of co-adsorbed solvent molecules could not be achieved.

III. Additional UV/vis absorption spectroscopy data

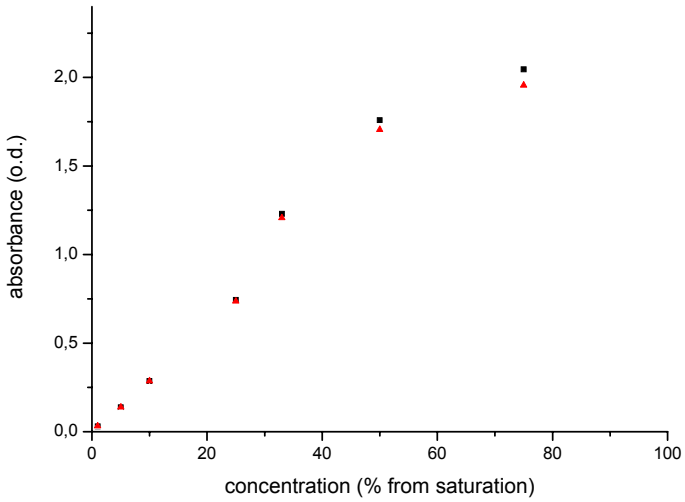

Figure S6. Lambert-Beer plot of molecule **I** dissolved in nonanoic acid. Black squares correspond to the absorbance at λ = 304 nm (aggregate related peak) and red triangles to the absorbance at λ = 323 nm (monomer related peak) (see also Fig. 3 main text). Absorbance is plotted as measured with a 1 mm cuvette.

IV. Theoretical Calculations

The Consistent Valence Force Field (CVFF) was applied to model monolayers of adsorbed molecules on graphite using the Cerius[2] (Version 4.5, MSI) software package. The use of the CVFF was motivated by previous works on structure optimization of organic monolayers on graphite.[1] Here, periodic boundary conditions were employed with the experimental unit cells as a constraint. The graphite substrate was approximated by two layers and atomic positions in the second layer were fixed. Values for the unit cell parameters were deduced from split images, where one part of the image depicts the adsorbate layer and in the other part the graphite substrate was atomically resolved. Molecules were arranged on the surface without further constraints. An energy difference of $< 2\times10^{-5}$ kcal/mol between single steps served as a convergence criteria.

The geometry of isolated molecules **I** and **II** was optimized using density functional theory (DFT) implemented in the Gaussian03 software package.[2] For this purpose, the B3LYP functional was used with the 6-31G(d) basis set. Convergence RMS force criterion was set to 3×10^{-4} Hartree/Bohr.

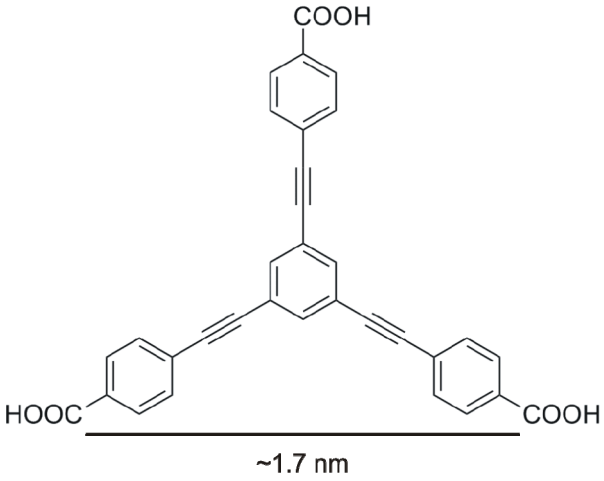

Figure S7. Schematic drawing indicating the distance between two carboxylic groups (carbon atoms were used as reference) of molecule **I** as calculated by DFT calculations.

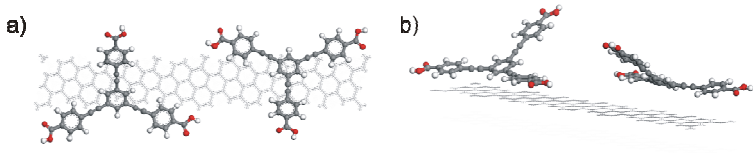

Figure S8. ***(a)*** Top view and ***(b)*** side view of a dimer of molecule **I** in the row structure on HOPG after geometry optimization by force-field calculation. Molecules in adjacent rows are tilted in opposite directions. The tilting angle of the molecule with respect to the substrate is ~36°. The distance of the upper phenyl ring of a molecule to the C-C triple bond of its intra-row neighbor accounts to ~3.7 Å which allows for aromatic interaction. Unit cell: 3.8 nm × 0.8 nm, 84°.

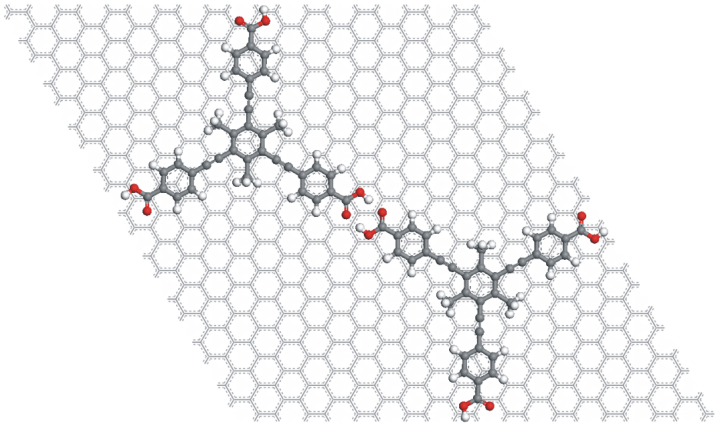

Figure S9. Top view of a dimer of molecule **II** on HOPG after geometry optimization by force-field calculations. Three pairs of hydrogen bonds per molecule stabilize the hexagonal structure. Unit cell: 4.1 nm × 4.1 nm, 60°.

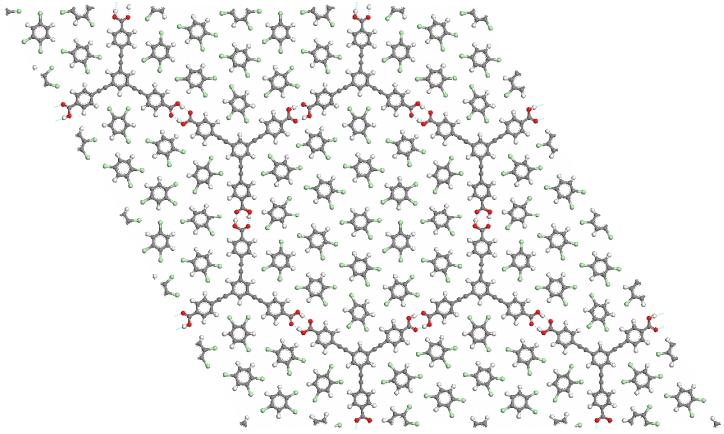

Figure S10. Force field calculation of a model with 19 co-adsorbed TCB solvent molecules within the cavities of an H-bonded network of molecule **I**. Four unit cells (4.1 nm × 4.1 nm, 60°).

V. References

1. Yin, S. X.; Wang, C.; Xu, Q. M.; Lei, S. B.; Wan, L. J.; Bai, C. L. *Chem. Phys. Lett.* **2001,** 348, (3-4), 321-328.
2. Frisch, M. J.; Trucks, G. W.; Schlegel, H. B.; Scuseria, G. E.; Robb, M. A.; Cheeseman, J. R.; Montgomery, J., J. A.; Vreven, T.; Kudin, K. N.; Burant, J. C.; Millam, J. M.; Iyengar, S. S.; Tomasi, J.; Barone, V.; Mennucci, B.; Cossi, M.; Scalmani, G.; Rega, N.; Petersson, G. A.; Nakatsuji, H.; Hada, M.; Ehara, M.; Toyota, K.; Fukuda, R.; Hasegawa, J.; Ishida, M.; Nakajima, T.; Honda, Y.; Kitao, O.; Nakai, H.; Klene, M.; Li, X.; Knox, J. E.; Hratchian, H. P.; Cross, J. B.; Bakken, V.; Adamo, C.; Jaramillo, J.; Gomperts, R.; Stratmann, R. E.; Yazyev, O.; Austin, A. J.; Cammi, R.; Pomelli, C.; Ochterski, J. W.; Ayala, P. Y.; Morokuma, K.; Voth, G. A.; Salvador, P.; Dannenberg, J. J.; Zakrzewski, V. G.; Dapprich, S.; Daniels, A. D.; Strain, M. C.; Farkas, O.; Malick, D. K.; Rabuck, A. D.; Raghavachari, K.; Foresman, J. B.; Ortiz, J. V.; Cui, Q.; Baboul, A. G.; Clifford, S.; Cioslowski, J.; Stefanov, B. B.; Liu, G.; Liashenko, A.; Piskorz, P.; Komaromi, I.; Martin, R. L.; Fox, D. J.; Keith, T.; Al-Laham, M. A.; Peng, C. Y.; Nanayakkara, A.; Challacombe, M.; Gill, P. M. W.; Johnson, B.; Chen, W.; Wong, M. W.; Gonzalez, C.; Pople, J. A., *Gaussian 03, Revision C.02,* **2004**, Gaussian, Inc., Wallingford CT, USA